

## Overview of the ITER EC H&CD system and its capabilities

T. Omori<sup>a,\*</sup>, M.A. Henderson<sup>a</sup>, F. Albajar<sup>b</sup>, S. Alberti<sup>c</sup>, U. Baruah<sup>d</sup>, T.S. Bigelow<sup>e</sup>, B. Beckett<sup>a</sup>, R. Bertizzolo<sup>c</sup>, T. Bonicelli<sup>b</sup>, A. Bruschi<sup>f</sup>, J.B. Caughman<sup>e</sup>, R. Chavan<sup>c</sup>, S. Cirant<sup>f</sup>, A. Collazos<sup>c</sup>, D. Cox<sup>a</sup>, C. Darbos<sup>a</sup>, M.R. de Baar<sup>g</sup>, G. Denisov<sup>h</sup>, D. Farina<sup>f</sup>, F. Gandini<sup>a</sup>, T. Gassmann<sup>a</sup>, T.P. Goodman<sup>c</sup>, R. Heidinger<sup>b</sup>, J.P. Hogge<sup>c</sup>, S. Illy<sup>i</sup>, O. Jean<sup>a</sup>, J. Jin<sup>i</sup>, K. Kajiwara<sup>j</sup>, W. Kasperek<sup>k</sup>, A. Kasugai<sup>j</sup>, S. Kern<sup>i</sup>, N. Kobayashi<sup>j</sup>, H. Kumric<sup>k</sup>, J.D. Landis<sup>c</sup>, A. Moro<sup>f</sup>, C. Nazare<sup>a</sup>, Y. Oda<sup>j</sup>, I. Pagonakis<sup>c</sup>, B. Piosczyk<sup>i</sup>, P. Platania<sup>f</sup>, B. Plaum<sup>k</sup>, E. Poli<sup>l</sup>, L. Porte<sup>c</sup>, D. Purohit<sup>a</sup>, G. Ramponi<sup>f</sup>, S.L. Rao<sup>d</sup>, D.A. Rasmussen<sup>e</sup>, D.M.S. Ronden<sup>g</sup>, T. Rzesnicki<sup>i</sup>, G. Saibene<sup>b</sup>, K. Sakamoto<sup>j</sup>, F. Sanchez<sup>c</sup>, T. Scherer<sup>i</sup>, M.A. Shapiro<sup>m</sup>, C. Sozzi<sup>f</sup>, P. Spaeh<sup>i</sup>, D. Strauss<sup>i</sup>, O. Sauter<sup>c</sup>, K. Takahashi<sup>j</sup>, R.J. Temkin<sup>m</sup>, M. Thumm<sup>i</sup>, M.Q. Tran<sup>c</sup>, V.S. Udintsev<sup>a</sup>, H. Zohm<sup>l</sup>

<sup>a</sup> ITER Organization, CS 90 046, 13067 St Paul Lez Durance Cedex, France

<sup>b</sup> Fusion for Energy, C/Josep Pla 2, Torres Diagonal Litoral-B3, E-08019 Barcelona, Spain

<sup>c</sup> CRPP-Association EURATOM-Confédération Suisse, EPFL Ecublens, CH-1015 Lausanne, Switzerland

<sup>d</sup> Institute for Plasma Research, Near Indira Bridge, Bhat, Gandhinagar 382428, India

<sup>e</sup> US ITER Project Office, ORNL, 055 Commerce Park, PO Box 2008, Oak Ridge, TN 37831, USA

<sup>f</sup> Istituto di Fisica del Plasma, Association EURATOM-ENEA-CNR, Milano, Italy

<sup>g</sup> Association EURATOM-FOM, 3430 BE Nieuwegein, The Netherlands

<sup>h</sup> Institute of Applied Physics, 46 Ulyanov Street, Nizhny Novgorod 603950, Russia

<sup>i</sup> Karlsruhe Institute of Technology, Association EURATOM-KIT, D-76021 Karlsruhe, Germany

<sup>j</sup> Japan Atomic Energy Agency (JAEA) 801-1 Mukoyama, Naka-shi, Ibaraki 311-0193, Japan

<sup>k</sup> Institut fuer Plasmaforschung, Universitaet Stuttgart, Pfaffenwaldring 31, D-70569 Stuttgart, Germany

<sup>l</sup> IPP-Garching, Association EURATOM-IPP, D-85748 Garching, Germany

<sup>m</sup> MIT Plasma Science and Fusion Center, Cambridge, MA 02139, USA

### ARTICLE INFO

#### Article history:

Available online 17 March 2011

#### Keywords:

ITER  
Electron Cyclotron  
MHD stabilization  
Launcher

### ABSTRACT

The Electron Cyclotron (EC) system for the ITER tokamak is designed to inject  $\geq 20$  MW RF power into the plasma for Heating and Current Drive (H&CD) applications. The EC system consists of up to 26 gyrotrons (between 1 and 2 MW each), the associated power supplies, 24 transmission lines and 5 launchers. The EC system has a diverse range of applications including central heating and current drive, current profile tailoring and control of plasma magneto-hydrodynamic (MHD) instabilities such as the sawtooth and neoclassical tearing modes (NTMs). This diverse range of applications requires the launchers to be capable of depositing the EC power across nearly the entire plasma cross section. This is achieved by two types of antennas: an equatorial port launcher (capable of injecting up to 20 MW from the plasma axis to mid-radius) and four upper port launchers providing access from inside of mid radius to near the plasma edge. The equatorial launcher design is optimized for central heating, current drive and profile tailoring, while the upper launcher should provide a very focused and peaked current density profile to control the plasma instabilities.

The overall EC system has been modified during the past 3 years taking into account the issues identified in the ITER design review from 2007 and 2008 as well as integrating new technologies. This paper will review the principal objectives of the EC system, modifications made during the past 2 years and how the design is compliant with the principal objectives.

© 2011 ITER Organization. Published by Elsevier B.V. All rights reserved.

### 1. Introduction

A powerful 24 MW Electron Cyclotron (EC) system [1,2] operating at 170 GHz with pulse lengths up to 3600 s is planned to be installed for the ITER tokamak that will be used for central heating and current drive (H&CD) applications as well as off-axis control of

\* Corresponding author. Tel.: +33 4 42 17 84 42.

E-mail address: [toshimichi.omori@iter.org](mailto:toshimichi.omori@iter.org) (T. Omori).

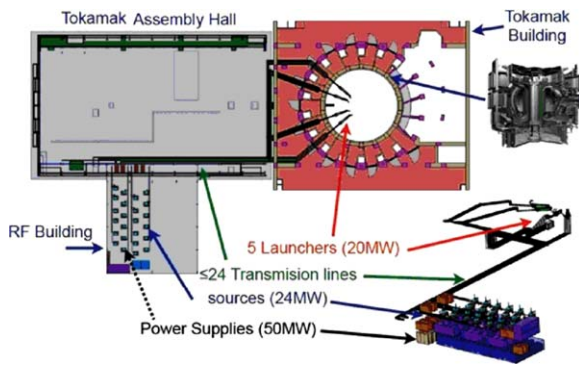


**Fig. 1.** The ITER EC system is divided into four subsystems, power supplies, gyrotrons, transmission lines and launchers. They are going to be procured from five DAs.

magneto-hydrodynamic (MHD) instabilities. Design work for the ITER EC system is moving forward with the following main functionalities:

- Assist initial breakdown and heat during current ramp-up.
- Provide auxiliary heating to assist in accessing H mode and achieve  $Q=10$ .
- Provide steady state on-axis and off-axis current drive in the range of  $0 < \rho_T < 0.45$  (where  $\rho_T$  is the square root of the normalized toroidal flux).
- Control MHD instabilities by localized current drive.
- Provide one-third of the total power for counter-ECCD in the range of  $0 < \rho_T < 0.45$ .
- Provide on/off power modulated from CW to 1 kHz and 50–100% power modulation from 1 to 5 kHz.

The EC system is comprised of four subsystems as follows: up to 26 gyrotrons (may include a couple of spares), matching high voltage power supplies (HVPS), 24 transmission lines (TL) and launchers. These subsystems are being designed and procured based on a partnership between the ITER organization (IO) and five Domestic Agencies (DAs) involved in the EC system development.

In general, the IO is responsible for the functional specifications of all components, the integration management, part of the installation, commissioning and operation. The fundamental layout for the whole EC system is illustrated in Fig. 1.

This paper provides an overview of the planned EC system, with a technical description based on physical requirements and the current status of design activities comparing these to the envisioned functional capabilities.

## 2. Design status and capabilities

The procurement of all subsystems is performed by the DAs. The HVPSs are designed, procured and installed by Europe and India. Development of the gyrotrons is being advanced by four DAs (Europe, India, Japan and Russia). Procurement, installation and commissioning of them will be made by each DA at the ITER site. The US develops and procures the TLs, which the IO installs and commissions. The launcher which is going to be deployed at the Equatorial port (EL) is procured by Japan and four launchers at the Upper ports (UL) by Europe. These launchers are installed and commissioned by the IO. The overall system is operated by the IO.

The in-kind procurement strategy taken to build the ITER EC system requires careful management by the IO of the interfaces between each sub-system and with interfacing services such as coolants, vacuum, buildings and so on [3]. The EC subsystems are to come as a complete package including cabling, control systems,

water manifolds, etc., such that all packages fit together without the IO procuring any components. The interface boundaries of the four EC subsystems procured by each DAs are shown in Fig. 2.

### 2.1. Power supplies

The EC high voltage power supplies [4–6] consist of a main power supply (MHVPS, 55 kV/90 A, up to 1 kHz modulation capability), body power supply (BPS, 35 kV, up to 5 kHz modulation capability) and anode power supply for the triode gyrotrons (APS, 40 kV, up to 5 kHz modulation capability). Each MHVPS generates sufficient electrical power for 2 MW microwave power source, with either one supply connected to two 1 MW or one 2 MW gyrotrons, whereas all gyrotrons have their own BPS (and APS for the 8 MW procured by Japan). All the power supplies shall ensure high voltage stability in ripple and accuracy of less than 1%. High efficiency of more than 97% is going to be achieved in the MHVPS development. Procurement allocation between India and Europe is in discussion.

### 2.2. Gyrotrons

The gyrotrons [7–12] are designed to generate 1 MW or more at the window output with an electrical efficiency of  $\geq 50\%$  and  $\geq 95\%$  coupling to the  $HE_{11}$  mode at the MOU (Matching Optic Unit). The gyrotron procurement includes a liquid helium free cryomagnet, MOU, cooling manifold, local control system, support structure, auxiliary power supplies and ancillary systems. All of the above equipment is housed in the RF building, which is compatible with a 24 MW EC system since it is dominated by the space required for the power supplies; i.e., they limit the number of installed gyrotrons to 24 under the assumption that all sources are 1 MW. The spacing is maximized within the finite size of the building to minimize stray magnetic field interference between neighboring gyrotrons. They will be distributed on a grid with typically  $\geq 5$  m spacing and an equivalent distance between building steel structures. All gyrotrons are positioned  $>90$  m from the tokamak center limiting the horizontal component of the stray magnetic field to  $\leq 3$  mT along the electron beam trajectory.

The procurement arrangement is scheduled to start in the summer of 2011 and the first delivery will be in 2015.

### 2.3. Transmission line

The corrugated waveguide transmission line [13–15] is designed to transmit the EC power from the gyrotrons up to the launcher diamond windows in the equatorial and upper port cells.

High  $HE_{11}$  mode purity at the input of the TL is essential to ensure the efficiency of the TL. Based on the calculation [16], the output power in the  $HE_{11}$  mode at the end of the TL will be decreased to around 0.92 times the fraction of input power in the  $HE_{11}$  mode from the incident beam power. The transmission line performs additional functions as follows:

- Monitor forward and reflected power (using power monitor mitre bend).
- Direct power to dummy load (via an in-line switch).
- Modify beam polarization for optimum plasma coupling.
- Deviate power to either upper or equatorial launchers.
- Provide pumping access for maintaining low pressure in line.
- Electrically isolate line from gyrotron and launchers.

As illustrated in Fig. 2, to achieve the above functionality, specific components such as switches, DC breaks, polarizers and so on have been included in the TL.

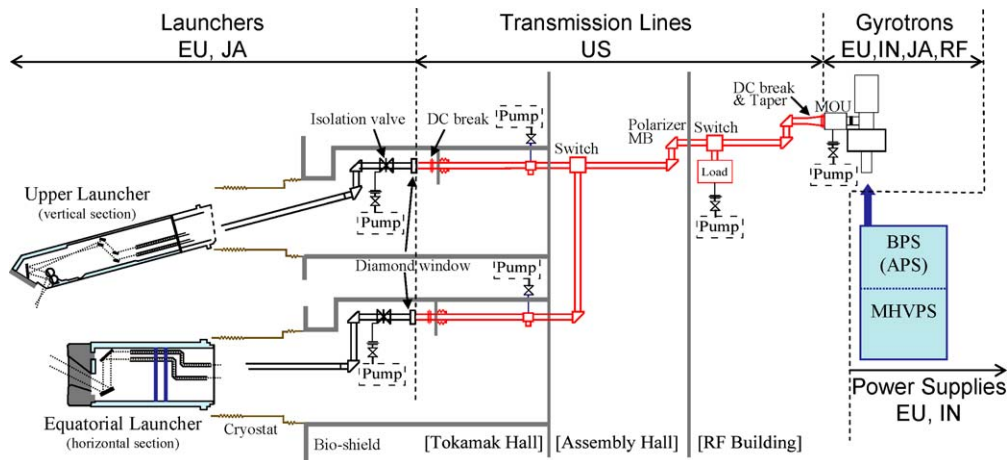


**Fig. 2.** Interfaces between the EC subsystems are defined as at the HV connectors at the gyrotron, the MOU output flange and the waveguide flange on the gyrotron side of the diamond window unit for their in-kind procurement. The interfaces with tokamak and buildings including utilities such as water cooling system, gases distribution and so on is managed by the IO.

The procurement arrangement has been signed in May 2010 and the first delivery will be in 2015.

2.4. Launchers

Two types of launchers are planned to achieve the required functionality of central H&CD and the off-axis CD for stabilizing MHD activity. These functions will be fulfilled by the right combinational use of the EL [17–19] and UL [20–22] which are shown in Figs. 3 and 4 respectively. Both launchers are to be compatible with 1.8 MW beams by taking into account 2 MW source operation (losses from MOU and TL will be >10%). As described in Fig. 2, each launcher is procured with the diamond window, isolation (or gate) valve and roughly 15 m length of ex-vessel waveguide. The diamond window and valve form the barriers in the first confinement system that prevents tritium and other material from traveling up the TL. The ex-vessel waveguide shall compensate for the torus displacements ( $\leq \pm 25$  mm) due to temperature variations, plasma disruptions, thermal quenches and loss of coolant.

The EL is going to be deployed at the equatorial port #14, has a total of 24 waveguides at the entry, which are grouped into three sets of eight beams. Each beam set is projected to a focusing mirror then to a flat steering mirror before passing through the blanket shield module (BSM) and into the plasma. The steering mir-

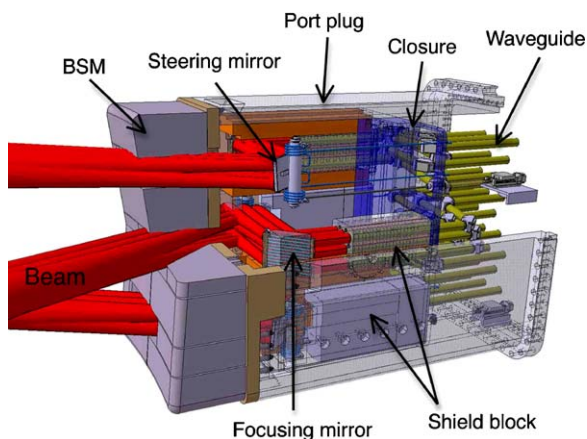


**Fig. 3.** The sectional view of the EL showing the waveguide orientation, focusing mirror, steering mirror, port plug structure and blanket modules.

ror directs the beam set in the toroidal direction from 20° to 40°, providing access from near on-axis to  $\rho_T \leq 0.45$ .

A total of four ULs are going to be deployed at the upper ports #12, 13, 15 and 16. Eight waveguide entries are grouped in two sets of four beams which follow free space propagation in the port plug through a set of four mirrors that regroup and focus the beams to provide a narrow and peaked current density profile for control of the MHD instabilities. An upper and a lower steering mirror injects the beam over a poloidal range of  $\pm 12^\circ$  to access the relevant  $q=2$  and  $3/2$  rational flux surfaces. The beams have a nearly fixed toroidal injection angle of about 20° that provides a maximized peak current density profile over the desired access range. For the ULs installed in the ports #12 and 13, a maximum of four beams can be injected such that the beam from the main TL is switched to waveguide entries for either the upper steering mirror or the lower steering mirror.

The functional capabilities of the EC system strongly depend on the focusing and access range provided by these two types of launchers. In a previous design, prior to 2007, the physics applications were partitioned between the two launchers based on regions of absorbed RF power into the plasma [23]. The EL had to access regions within of  $\rho_T \leq \sim 0.45$  for applications associated with central heating, current drive and sawtooth control, and the ULs could access only the region where NTMs would be expected to occur between  $\sim 0.55 \leq \rho_T \leq \sim 0.85$ . Therefore, the combination of two launchers could not achieve the presently desired accessibility.

The design has been modified to increase the access range and avoid regions of non-accessibility on the launchers by increasing

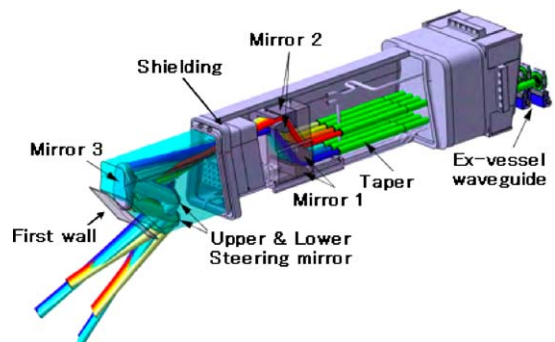


**Fig. 4.** The sectional view of the UL showing the waveguide orientation, three fixed mirror sets, two steering mirrors, port plug structure and blanket modules.

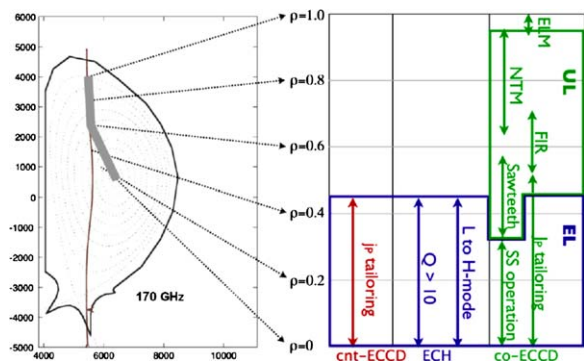


**Fig. 5.** The revised EL and UL access nearly the entire plasma cross section and are capable of injecting 20 MW in the co-ECCD direction, 6.7 MW in the counter-ECCD, or a balanced injection of the full 20 MW for pure heating.

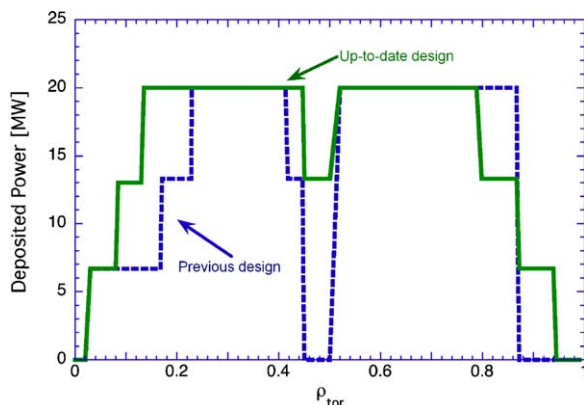


**Fig. 6.** The maximum power that can be deposited at any given location in the plasma cross section based on the previous design (dashed line) and up-to-date configuration (solid line).

the access range of the UL. As shown in Figs. 5 and 6, the physics applications have been repartitioned between the two launchers [24], dividing the functional requirements based on the need for broad (EL) or narrow (UL) deposition profiles. The EL will still be used for central heating and current drive applications [25], while the UL is used for the control of both the NTM and sawtooth instabilities. In addition, one third of the EL beams are to provide counter current drive to decouple the heating and current drive contributions when depositing power centrally.

### 3. Future prospects

The EC system is envisioned to generate 8 MW RF power for the first ITER plasma operation scheduled in November 2019 and the

full 24 MW for the second operating period in late 2021. The design, manufacturing, installation and commissioning activities are configured according to these milestones with some margin of float (typically more than a year) prior to the planned plasma initiation date. The installation process will begin in early 2015 when the RF, assembly and tokamak buildings are available for EC equipment installation.

### References

- [1] C. Darbos, M. Henderson, *Fusion Eng. Des.* 84 (2009) 651.
- [2] M. Henderson, The ITER EC H&CD system, in: EC-16 Meeting, Sanya, China, 12–15 April, 2010.
- [3] M. Henderson, G. Saibene, *Nucl. Fusion* 48 (2008) 054017.
- [4] D. Fasel, T. Bonicelli, M.A. Henderson, M.Q. Tran, *Fusion Sci. Technol.* 53 (2008) 246.
- [5] T. Gassmann, B. Beaumont, U.K. Baruah, T. Bonicelli, S. Chiochio, D. Cox, et al., Integration of IC/EC systems in ITER, *Fusion Eng. Des.* 85 (2010) 1245.
- [6] T. Gassmann, B. Arambhadiya, B. Beaumont, U.K. Baruah, T. Bonicelli, C. Darbos, et al., High voltage power supplies for ITER RF heating and current drive systems, in: 26th SOFT, Porto, Portugal, 27 September–1 October, 2010.
- [7] K. Sakamoto, A. Kasugai, K. Takahashi, R. Minami, N. Kobayashi, K. Kajiwara, *Nat. Phys.* 3 (2007) 411.
- [8] G. Denisov, Recent development results in Russia of megawatt power gyrotrons for plasma fusion installations, in: EC-16 Meeting, Sanya, China, 12–15 April, 2010.
- [9] A.K. Sinha, et al., Design and development activities of gyrotrons in India, in: 5th IAEA Tech. Meeting “ECRH Physics and Tech. for Large Fusion Devices”, Gandhinagar, India, 18–20 February, 2009.
- [10] F. Albajar, The European 2 MW gyrotron for ITER, in: EC-16 Meeting, Sanya, China, 12–15 April, 2010.
- [11] J.P. Hogge, T. Goodman, S. Alberti, F. Albajar, K.A. Avramides, P. Benin, et al., *Fusion Sci. Technol.* 55 (2009) 204.
- [12] T. Rzesnicki, B. Piosczyk, S. Kern, S. Illy, J. Jianbo, A. Samartsev, A. Schlaich, M. Thumm, *IEEE Trans. Plasma Sci.* 38 (2010) 1141.
- [13] D. Rasmussen, R&D progress on the ITER EC transmission line, in: EC-16 Meeting, Sanya, China, 12–15 April, 2010.
- [14] D.M.S. Ronden, M.A. Henderson, B. Beckett, T. Bigelow, J. Caughman, C. Darbos, et al., The engineering analysis in support of the ITER ECH H&CD transmission lines, *Fusion Sci. Technol.* 59 (2011).
- [15] F. Gandini, T.S. Bigelow, B. Beckett, J.B. Caughman, D. Cox, C. Darbos, et al., The EC H&CD transmission line for ITER, *Fusion Sci. Technol.* 59 (2011).
- [16] M.A. Shapiro, E.J. Kowalski, J.R. Sirigiri, D.S. Tax, R.J. Temkin, T.S. Bigelow, J.B. Caughman, D.A. Rasmussen, *Fusion Sci. Technol.* 57 (2010) 196.
- [17] K. Takahashi, K. Kajiwara, N. Kobayashi, A. Kasugai, K. Sakamoto, *Nucl. Fusion* 48 (2008) 054014 (9 pp.).
- [18] K. Kajiwara, K. Takahashi, N. Kobayashi, A. Kasugai, K. Sakamoto, *Fusion Eng. Des.* 84 (2009) 72.
- [19] K. Takahashi, K. Kajiwara, Y. Okazaki, Y. Oda, K. Sakamoto, T. Omori, M. Henderson, Progress of ITER equatorial electron cyclotron launcher design for physics optimization and toward final design, in: 26th SOFT, Porto, Portugal, 27 September–1 October, 2010.
- [20] D. Strauss, Deflections and vibrations of the ITER ECRH upper launcher, in: EC-16 Meeting, Sanya, China, 12–15 April, 2010.
- [21] T. Scherer, Recent upgrades of the ITER ECRH CVD torus diamond window design and investigation of dielectric diamond properties, in: EC-16 Meeting, Sanya, China, 12–15 April, 2010.
- [22] M. Henderson, R. Heindinger, D. Strauss, R. Bertizzolo, A. Bruschi, R. Chavan, et al., *Nucl. Fusion* 48 (2008) 054013.
- [23] N. Kobayashi, G. Borgia, B. Petzold, *Fusion Eng. Des.* 53 (2001) 475.
- [24] G. Ramponi, D. Farina, M.A. Henderson, E. Poli, O. Sauter, G. Saibene, H. Zohm, C. Zucca, *Nucl. Fusion* 48 (2008) 054012.
- [25] C. Zucca, O. Sauter, M.A. Henderson, E. Fable, D. Farina, A. Polevoi, Theory of fusion plasmas, in: AIP Conf. Proc., vol. 1069, 2008, p. 361.